European Journal of Computational Mechanics, 2013
Vol. 22, Nos. 2–4, 120–131, http://dx.doi.org/10.1080/17797179.2013.820898

Taylor & Francis
Taylor & Francis Group

Dynamic model of high speed machining spindle associated to a self-vibratory drilling head influence of drill torsional-axial coupling

S.G. Mousavi*, V. Gagnol and P. Ray

Clermont Université, Institut Pascal, UBP-CNRS-IFMA, Campus des Cézeaux 24 Avenue des Landais, 63177, Aubiere Cedex, France

The drilling of deep holes with small diameters remains an unsatisfactory technology, since its productivity is rather limited. The main limit to an increase in productivity is directly related to the poor chip evacuation, which induces frequent tool breakage and poor surface quality. Retreat cycles and lubrication are common industrial solutions, but they induce productivity and environmental drawbacks. An alternative response to the chip evacuation problem is the use of a vibratory drilling head, which enables the chips to be fragmented thanks to the axial self-excited vibration. Contrary to conventional machining processes, axial drilling instability is sought, thanks to an adjustment of head design parameters and appropriate conditions of use. In this paper, self-vibratory cutting conditions are established through a specific stability lobes diagram. A dynamic high-speed spindle/drilling head/tool system model is elaborated on the basis of rotor dynamics predictions. The model-based tool tip Frequency Response Function (FRF) is integrated into an analytical stability approach. The torsional-axial coupling of the twist drill is investigated and consequences on drilling instability are established.

Keywords: self-vibratory drilling; machine tool dynamics; stability prediction; chatter analysis; machining prediction

1. Introduction

The drilling of deep, small-diameter holes is an unsatisfactory machining operation that results in poor surface quality and low productivity. These drawbacks are mainly related to difficulties in evacuating the chips through the drill flute during the cut. Non-productive retreat cycles and the use of high-pressure lubrication are the current industrial solutions used to evacuate chips but present, respectively, productivity and environmental problems. New drilling techniques have emerged, based on the tool's axial vibration, in order to fragment the chips and enhance their evacuation without the need for lubricants and retreat cycles. The two major technologies are:

- Vibration-assisted drilling technologies, based on forced excitations generated by a specific system implemented in the tool holder.
- Self-vibratory drilling technology, which uses the cutting energy to generate tool axial vibration (Guibert, Paris, & Rech, 2008). A specific self-vibratory drilling head (SVDH) excites low-energy chatter vibration for specific process parameters

*Corresponding author. Email: Said.Mousavi@ifma.fr

© 2013 Taylor & Francis

by using a combination of a low-rigidity axial spring and an additional mass located between the spindle and the tool. The self-excited vibrations must be tuned and controlled in order to have a magnitude greater than the feed per tooth, which enables the fragmentation of the chips without external adjunction of energy.

In this paper an original approach to establishing accurate stability lobes diagram in self-excited drilling operations is proposed. The predicted speed-dependent transfer function of the overall system, composed of spindle-SVDH-twist drill, is then integrated into an analytical chatter vibration stability approach to calculate the associated dynamic stability lobes diagram.

In the second section, the spindle-SVDH rotor dynamics model is presented. A special rotor-beam element, developed in a corotational reference frame (Gagnol et al., 2007a) is implemented. The rolling bearing stiffness matrices are calculated around a static function point on the basis of T.C Lim's formulation (Lim & Singh, 1990) and then integrated into the global finite element model. The rotating system is derived using *Timoshenko* beam theory. The identification of contact dynamics in tool-SVDH-spindle assemblies is carried out using the receptance coupling method on the basis of experimental substructure characterisation (Forestier, Gagnol, Ray, & Paris, 2011). The identified models are then integrated into the global spindle-SVDH-tool model.

In Section 3, a generic accurate drilling force model is developed by taking into account the drill geometry, cutting parameters and effect of torsion on the thrust force. Section 4 is dedicated to the prediction of adequate drilling conditions based on controlled self-excited drill vibration. A specific instability lobes diagram is elaborated by integrating into an analytical stability analysis the overall structural model-based tool tip Frequency Response Function (FRF) of the system associated with the proposed drilling force model. Investigations are focused on the drill's torsional-axial coupling role on instability predictions. Finally, a conclusion is presented.

2. Model building

The vibratory drilling system is composed of a SVDH body clamped to the spindle by a standard HSK63A tool-holder interface. A SVDH vibrating subsystem is jointed to the SVDH body using a specific spring, and axially guided by a ball retainer. Finally, a long drill is held in the SVDH vibrating subsystem with a standard ER25 collet chuck. The SVDH system is mounted on a spindle capable of speeds up to 15,500 rpm. The spindle has four angular bearings in overall back-to-back configuration (Figure 1). The spindle-SVDH-tool system is composed of four structural subsystems: the drill, the SVDH vibrating subsystem, the SVDH body and the spindle.

2.1. Structural elements

The model for the spindle-SVDH-tool system is restricted to the rotating structure composed of the spindle shaft, the SVDH and the drill. This hypothesis was established by an experimental modal identification procedure carried out on spindle substructure elements (Gagnol et al., 2007b). The motion of the rotating structure is considered as the superposition of rigid and elastic body displacements (Figure 2). Dynamic equations were obtained using *Lagrange* formulation associated with a finite element method. Due to the size of the rotor sections, shear deformations had to be taken into account.

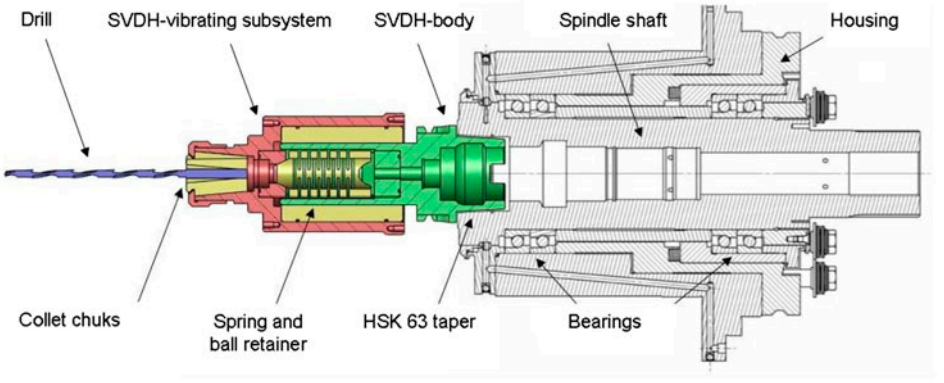

Figure 1. The spindle-SVDH-tool system.

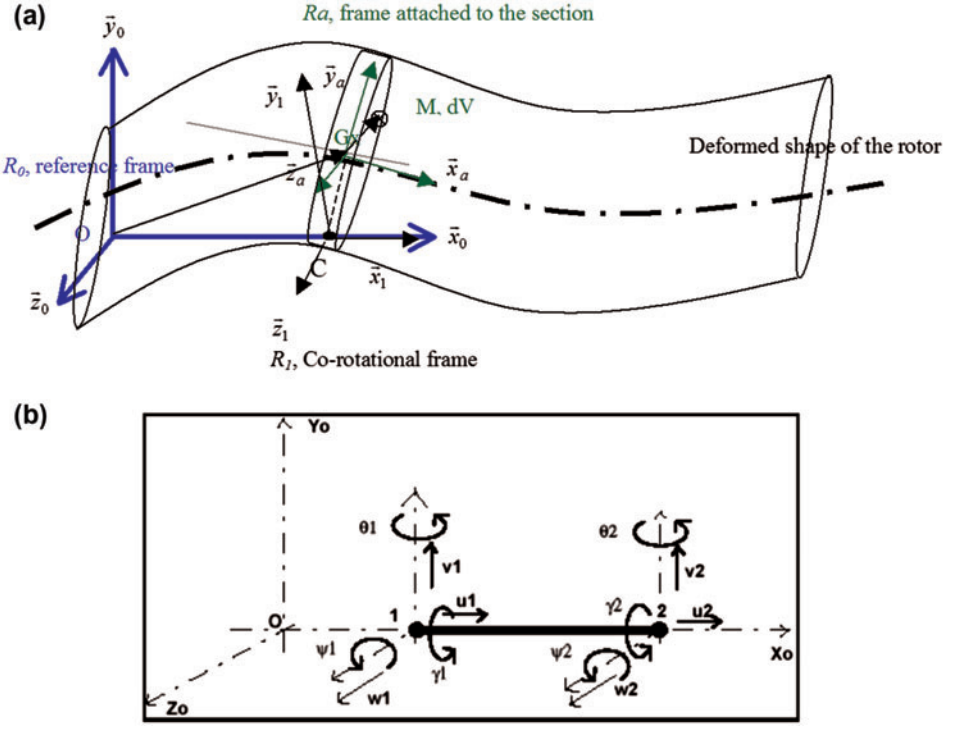

Figure 2. Reference frames used: (a) differential section kinematics and (b) beam element degrees of freedom.

Then, the rotating substructure was built using *Timoshenko* beam theory. The relevant shape functions were cubic in order to avoid shear-locking. A special three-dimensional rotor-beam element with two nodes and six degrees of freedom per node was developed in the corotational reference frame.

The damping model used draws on *Rayleigh* viscous equivalent damping, which makes it possible to regard the damping matrix **D** as a linear combination of the mass matrix **M** and the spindle rigidity matrix **K**:

$$\mathbf{D} = \alpha\mathbf{K} + \beta\mathbf{M} \tag{1}$$

where α and β are damping coefficients.

The set of differential equations can be written as follows:

$$\mathbf{M}\ddot{\mathbf{q}}_N + (2\Omega\mathbf{G} + \mathbf{D})\dot{\mathbf{q}}_N + (\mathbf{K} - \Omega^2\mathbf{N})\mathbf{q}_N = \mathbf{F}(t) \tag{2}$$

where **M** and **K** are the mass and stiffness matrices, **D** is the viscous equivalent damping matrix, $\mathbf{q}_N$ and $\mathbf{F}(t)$ are the nodal displacement and force vectors. **G** and **N** are, respectively, representative of gyroscopic and spin softening effects. Ω is the rotor's angular velocity.

2.2. *Modelling angular contact ball bearings*

The rotating system is supported by four (two front and two rear) hybrid angular contact bearings. The rolling bearings stiffness matrices were calculated using in-house software developed on the basis of T.C Lim's formulation (Lim & Singh, 1990). The bearing stiffness model represents the load-displacement relation combined with the Hertzian contact stress principle and is calculated around a static function point characterised by the bearings preload. Based on Rantatalo's prediction (Rantalalo, Aidanpaa, Goransson, & Norman, 2007), the initially calculated bearing stiffness is spindle speed-dependent because of the gyroscopic and centrifugal force **Fc**, which acts on each ball (Figure 3(a)). As the speed increased, the load conditions between the balls and the rings in the bearing changed because of the centrifugal force (Figure 3(a)). Then, speed-dependent bearing stiffness was integrated into the global spindle FEM and influenced the natural frequencies of the spindle-SVDH-tool unit under consideration.

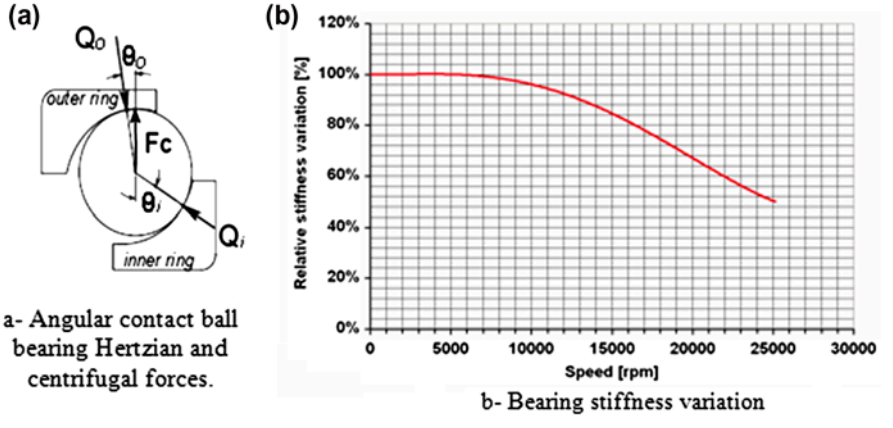

Figure 3. Bearing stiffness variation depending on spindle speed.

2.3. Modelling of spindle-SVDH-tool interfaces

The dynamic behaviour of the interfaces represented by the HSK63 taper, spring and ball retainer, and collet chuck are taken into account (Figure 1). The identification procedure of the interface models was carried out by Forestier (Forestier et al., 2011) based on the receptance coupling method and then integrated into the model as illustrated in Figure 4.

The axial dynamic behaviour of the interface is modelled by a spring-damper element whose transfer function is:

$$H_{interface}(\Omega) = \frac{1}{k + ic\Omega} \tag{3}$$

The rigidity k and damping c values were determined by minimising the gap between the measured and the modelled tool tip node frequency response function for a non-rotating spindle, using an optimisation routine and a least-squares type object function.

2.3.1. Model assembly and experimental validation

As in a classic finite element procedure, dynamic equations of the overall system, composed of the drill, the SVDH vibrating subsystems, the SVDH body and the spindle, were obtained by assembling element matrices. Matrices and vectors for each individual element are formed first and then linked together into a set of system equations. The spring-damper connection parameters between the drill and the SVDH vibrating subsystems and between the SVDH vibrating subsystems and SVDH body, identified by the receptance coupling method, enabled the rotor-beam models of the components to be assembled. The rolling bearing model imposes the boundary conditions of the system.

The spindle-SVDH-tool assembled model was validated by comparison between numerical and experimental FRF, as shown in Figure 5.

Figure 5 represents experimental and numerical axial FRF of the assembled system. The 60 and 4700 Hz modes are, respectively, due to the spring-ball retainer and collet chuck interfaces determined in the previous subsystem identification procedure. Some parasitical experimental bending modes at 193, 1237 and 2433 Hz are present in the experimental FRF.

A good correspondence between the numerical and experimental axial FRF curves enabled the numerical model to be used for further investigations.

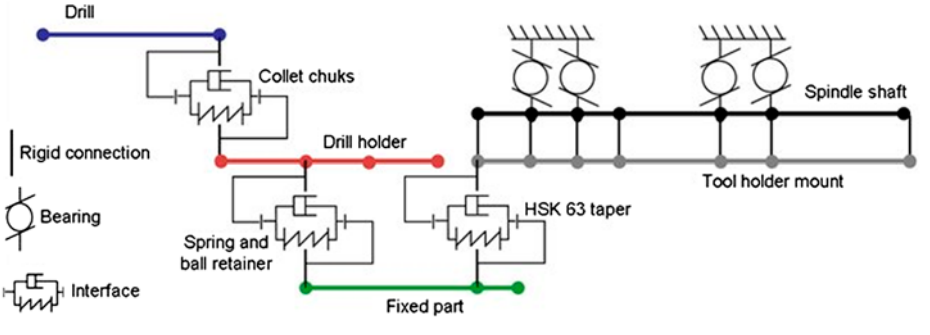

Figure 4. The spindle-SVDH-tool System Finite Element Model.

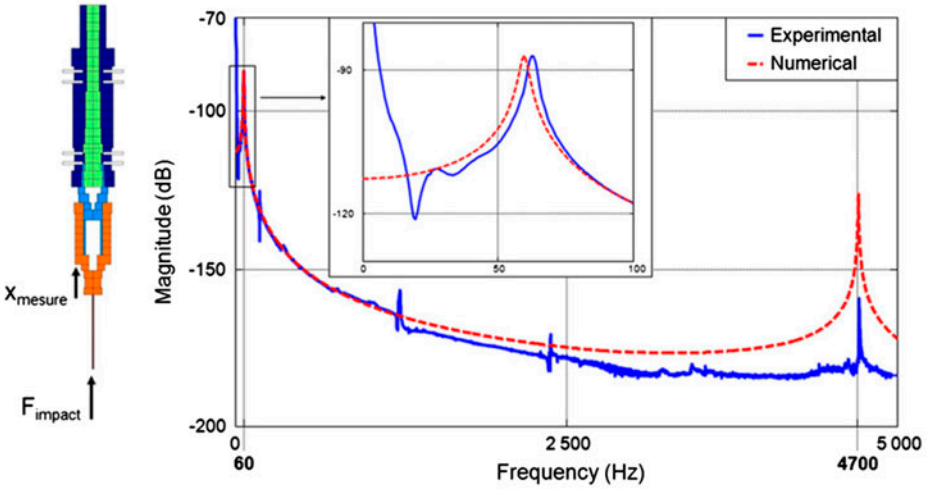

Figure 5. Numerical vs. experimental system axial FRF.

3. Drilling force model

The energy required to maintain the self-excited vibration is provided by the cutting forces. These excite both the SVDH and the flexible low-diameter drill. The combination of rigid body motion and dynamic displacements of the drill induces mainly torsional and axial vibrations.

Several force models have been proposed in the literature for the primary cutting edge presented in Figure 4 in zone 1. Both geometrical parameters and cutting pressures change greatly along the cutting lip of the twist drill (Roukema & Altintas, 2006). Each cutting lip can be thought of as being composed of a number of small differential segments. The elementary tangential force *dFt* is perpendicular to the cutting edge and the axial force *dFz* is in the drill axial direction. The cutting forces, axial forces and torque applied to the drill are evaluated by summing the elementary forces and torques acting on the basic elements of the edge of the drill and are expressed as a function of chip thickness h and width b.

Following Tlusty (1985) and Stephenson and Agapiou (1992), the net variations in the time-varying part of tangential and thrust forces at the drill tip are assumed to be proportional to the chip area. The influence of the ploughing effect and the effect of the chisel edge are not taken into account in the proposed cutting force model. Hence, the thrust force, the axial force and the torque at the tool tip are, respectively:

$$\begin{aligned} F_t &= \sum_i dF_t = -K_t bh \\ F_Z &= \sum_i dF_Z = -K_Z bh \\ M_Z &= 2\sum dF_t \times r(z) = -K_t bhR_{av} \end{aligned} \tag{4}$$

where R_{av} is the average radius of the cutting force, h is the chip thickness and b is the radial depth of cut (drill diameter minus pilot hole diameter, if there is a pilot hole). K_z and K_t are the average cutting pressures in the axial and tangential directions, respectively.

3.1. Torsional-axial coupling

The development of a torsional-axial vibration model (Bayly and Metzer 2001) was a major milestone in understanding chatter in machining using a twist drill. The torsional-axial theory of Bayly is based on the fact that when a twist drill "untwists", it extends in length (Figure 5).

Twisting and axial deformations are coupled. Accordingly, the second member of Equation (2) becomes:

$$F(t) \times \vec{z} = -F_z(t) - (\theta)M_Z(t) \tag{5}$$

The θ term represents a torsional-axial coupling parameter, since it relates the applied torque to drill axial excitation. It is determined by FEM analysis (Figure 5(b)). The coupling is negative, since when the drill twists in -z resulting from the negative cutting torque it also extends in $+z$ which results in a negative axial force contribution. According to Equation (3), Equation (4) can be rewritten as follows:

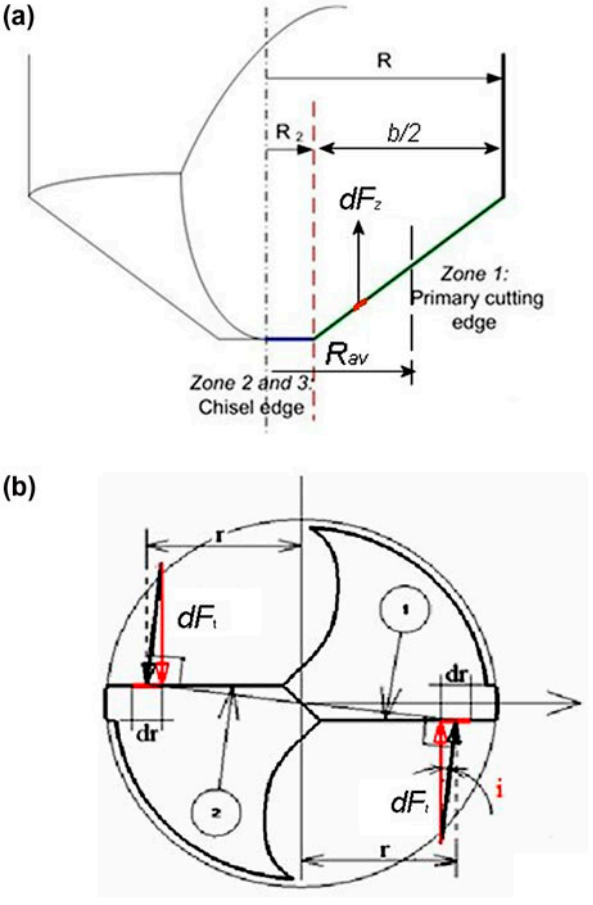

Figure 6. Drill geometry, elementary forces.

$$F(t) \times \vec{z} = h \times b \times K_t \times \alpha \text{ with } \alpha = \frac{K_Z}{K_t} + R_{av} \times \theta \quad (6)$$

K_z and K_t are identified through experimental drilling characterisation (Guibert et al. 2008), and the coupling term $R_{av}\theta$ by finite element modelling of the drill. In our case, using a carbide drill of 5 mm diameter, the helix angle is 30° and the material to be machined is 35MnV7. The identification of terms $R_{av}\theta$ and α is, respectively, .45 and .39.

4. Stability prediction

Torsional-axial coupling in the drill and SVDH vibration provide a mechanism for torsional-axial chatter. The torsional vibrations lead to the shortening and lengthening of the drill, which results in a wavy surface of the bottom of the hole. The main difficulty of vibratory drilling is to foresee the cutting conditions that will generate regular vibrations able to induce interrupted cutting. In this study, the drilling operation is considered

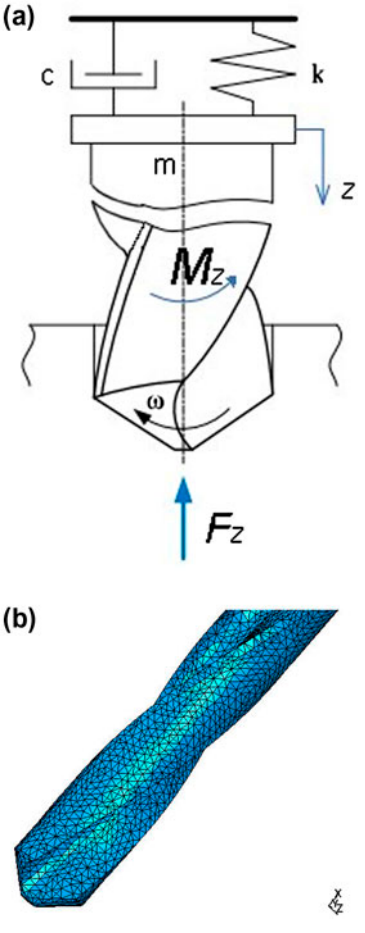

Figure 7. (a) Dynamic model of drill bit (b) Finite element model of the drill.

as having one degree of freedom in thrust force, taking into account the torsion effect in this direction (Figure 7). The analytical method allows the stability of system to be investigated from the study of the chip thickness (Figure 8(a)). The regenerative chatter of system can be presented by the block diagram shown in Figure 8(b).

The cutting forces and coupling term, Equation (5), are substituted into Equation (2) for motion in the drill's axial direction:

$$(\mathbf{M}\ddot{\mathbf{q}}_N + (2\Omega\mathbf{G} + \mathbf{D})\dot{\mathbf{q}}_N + (\mathbf{K} - \Omega^2\mathbf{N})\mathbf{q}_N) \times \vec{z} = \alpha K_t b(Z(t) - Z(t-\tau)) \tag{7}$$

The chip thickness, due to regenerative displacement, is expressed in the Laplace domain:

$$h(s) = f_z + Z(s) - Z(s)e^{-sT} \tag{8}$$

where f_z is the feed rate per tooth and T is the tooth period. $Z(s)$ is the axial tool tip displacement.

The stability diagram is obtained by integrating the numerical-predicted axial tool tip frequency response into the chatter stability approaches. The axial transfer function $H(j\omega)$ representing the ratio between the Fourier transform of the axial displacement $Z(j\omega)$ at the tool tip and the axial dynamic cutting force $F(j\omega)$ is expressed as follows:

$$H(j\omega) = \frac{x(j\omega)}{F(j\omega)} = inv(-\mathbf{M}\omega^2 + (2\Omega\mathbf{G} + \mathbf{D})\omega + (\mathbf{K} - \Omega^2\mathbf{N})) \tag{9}$$

$H(j\omega) = R(\omega) + jI(\omega)$ where R and I are, respectively, the real part and the imaginary part of the transfer function. They depend on the adjustable parameter of the SVDH, i.e. the axial spring rigidity and the additional SVDH mass.

For a given axial SVDH rigidity or SVDH mass, the chip thickness can be expressed as follows:

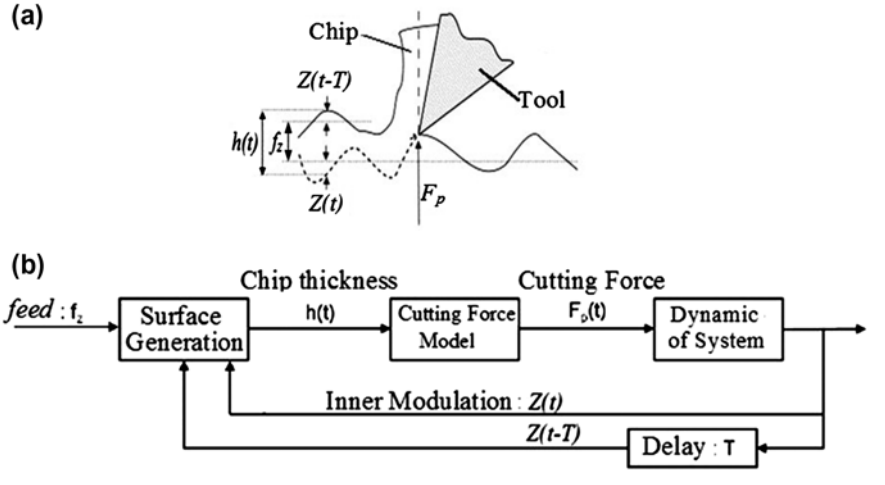

Figure 8. (a) dynamic chip thickness (b) block diagram of chatter dynamics.

$$h(s) = \frac{f_z}{1 + \alpha K_t DZ(R(s) + iI(s))(1 - e^{-sT})} \tag{10}$$

The resulting stability relationships (Equations (9) and (10)) are obtained, at the stability limit: $s = i\omega_c$, by annulling, respectively, the real part and the imaginary part of Equation (8)'s denominator.

$$1 + 2\alpha K_t DZR(\omega_c) = 0 \tag{11}$$

$$N = \frac{60\omega_c}{Z(2\varphi + 3\pi + 2p\pi)} \quad \text{with: } \varphi = \tan^{-1}\left(\frac{I(\omega_c)}{R(\omega_c)}\right) \tag{12}$$

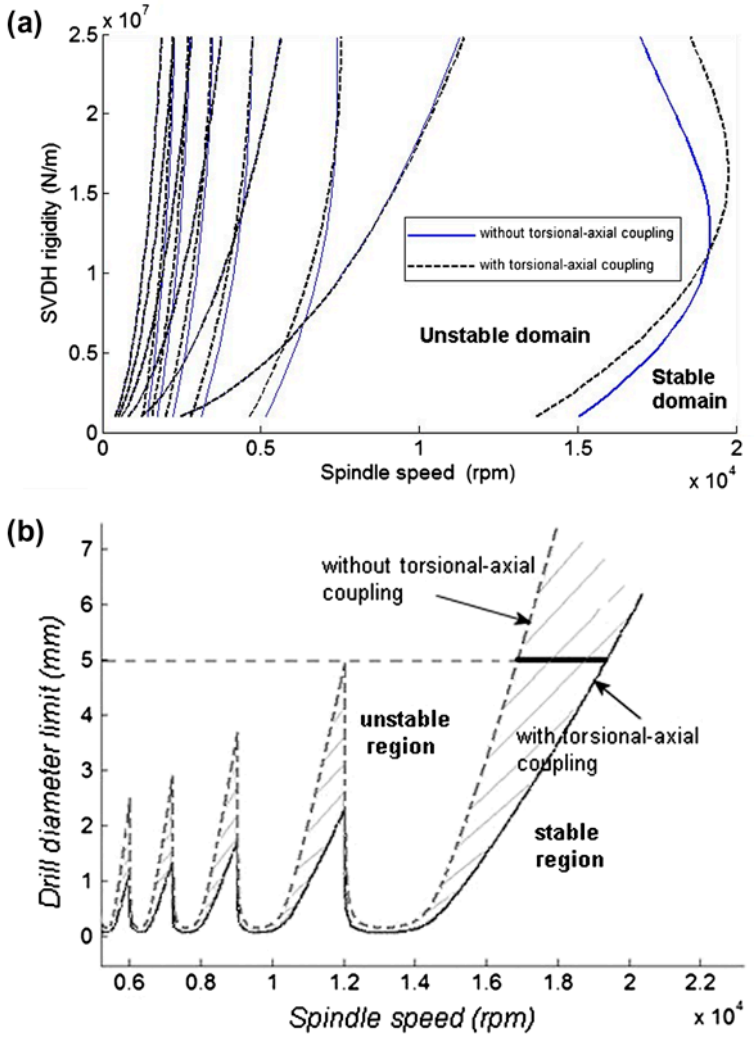

Figure 9. Stability lobes with and without torsional-axial coupling.

The stability limit, integrating drill torsional-axial vibration, can be established:

$$D_{\text{lim}} = \frac{-1}{\alpha \times K_t \times 2 \times R(\omega)} \tag{13}$$

where $R(\omega)$ is the real part of the global system (Spindle-SVDH-drill) transfer function. α is the torsional-axial coupling term (Equation (5)). The stiffness and mobile mass of the SVDH are adjustable and require tuning to optimise the process. The stability lobes in a drilling operation can be established (Figure 9).

Figure 9(a) represents the computed stability diagrams in the plane of spindle speed and SVDH stiffness. It can be noticed that the torsional-axial coupling effect influences the instability of the process, depending on SVDH rigidity. Figure 9(b) represents stability predictions in the plane of spindle speed and drill diameter. It is established for SVDH rigidity of up to 1.2e7 Nm, where the operating domain representative of self-excited vibrations is increased. For a drilling operation with a 5 mm diameter drill, the maximum spindle speed is increased from 16,800 to 19,500 rpm by taking into account the torsional-axial coupling of the drill.

5. Conclusion

The use of SVDH to drill small-diameter deep holes enables productivity to be improved by eliminating the retreat cycles. The main difficulty is to choose the adequate cutting parameters to obtain self-excited vibrations that enable the fragmentation of the chips. To achieve this goal, a dynamic model of the global system composed of spindle–SVDH-tool is developed. The structural components of the system were modelled using a specific rotor-beam element, taking into account the speed-dependent gyroscopic effects and centrifugal forces. The interface models were identified by the receptance coupling method and then integrated into the global spindle-SVDH-tool model.

Adequate cutting conditions are determined by integrating the model-based tool tip transfer function into an analytical chatter vibration stability approach. Specific stability lobe diagrams are elaborated, taking into account the effective dynamic properties of the studied system. The torsional-axial coupling of the twist drill is modelled based on Bayly's approach and integrated into the overall system dynamics in order to investigate drilling stability. The stability lobes established indicate modifications of self-excited operating zones, allowing increased drilling operation productivity for specifics combinations of SVDH rigidity and mass. Taking into account the torsional-axial coupling of the drill allows refining the stability prediction of the global system during a drilling operation.

References

Bayly, P. V., & Metzler, S. A. (2001). Theory of torsional chatter in twist drills: Model, stability analysis and composition to test. *Journal of Manufacturing Science and Engineering, 123*, 552–561.

Forestier, F., Gagnol, V., Ray, P., & Paris, H. (2011). Model-based operating recommendations for high-speed spindles equipped with a self-vibratory drilling head. *Journal of Mechanism and Machine Theory, 46*, 1610–1622.

Gagnol, V., Bouzgarrou, C. B., Ray, P., & Barra, C. (2007a). Model-based chatter stability prediction for high-speed spindles. *International Journal of Machine Tools and Manufacture, 47*, 1176–1186.

Gagnol, V., Bouzgarrou, B. C., Ray, P., & Barra, C. (2007b). Rotor dynamics based chatter prediction in milling and spindle design optimization. *ASME Journal of Manufacturing Science and Engineering, 129*, 407–415.

Guibert, N., Paris, H., & Rech, J. (2008). A numerical simulator to predict the dynamical behavior of the self vibratory drilling head. *International Journal of Machine Tools and Manufacture, 48*, 644–655.

Lim T. C., & Singh R. (1990). Vibration transmission throught rolling element bearings, Part I to Part III. *Journal of Sound and Vibrations, 139*, 179–199, 201–225.

Rantalalo, M., Aidanpaa, J. O., Goransson, B., & Norman, V. (2007). Milling machine spindle analysis using FEM and non-contact spindle excitation and response measurement. *International Journal of Machine Tools and Manufacture, 47*, 1034–1045.

Roukema, J. C., & Altintas, Y. (2006). Generalized modeling of drilling vibration, Part I: Time domain model of drilling kinematics, dynamics and hole formation. *International Journal of Machine Tools & Manufacture, 46*, 2073–2085.

Stephenson, D. A., & Agapiou, J. S. (1992). Calculation of main cutting edge forces and torque for drills with arbitrary point geometries. *International Journal of Machine Tools and Manufacture, 32*, 521–538.

Tlusty, J. (1985). Machine dynamics, handbook of high-speed machining technology. In R. I. King (Ed.), New York: Chapman and Hall.